RESEARCH ARTICLE

Radiolaria and Phaeodaria (siliceous Rhizaria) in south-western and northern Norwegian fjords during late summer 2016: dominant species and biomass in shallow-water assemblages

Takahito Ikenoue[1], Kjell R. Bjørklund[2], Anders K. Krabberød[3], Shigeto Nishino[1] & Paul Wassmann[4]

[1]Research Institute for Global Change, Japan Agency for Marine-Earth Science and Technology, Yokosuka, Japan; [2]Natural History Museum, University of Oslo, Oslo, Norway; [3]Department of Biosciences, Centre for Integrative Microbial Evolution and Centre for Epigenetics Development and Evolution, University of Oslo, Oslo, Norway; [4]Department of Arctic and Marine Biology, UiT The Arctic University of Norway, Tromsø, Norway

Abstract

To determine the present-day community composition of siliceous Rhizaria (Radiolaria and Phaeodaria) in Norwegian fjords, plankton tows were conducted in south-western and northern Norwegian fjords in September 2016. The mean total abundance of radiolarians was 306 m^{-3} in the Sognefjord complex, which was the southern research site, and, in the north, 945 m^{-3} in Malangen and 89 m^{-3} in Balsfjord, both above the Arctic Circle. *Sticholonche zanclea* was the most abundant radiolarian in the Sognefjord complex and Malangen, accounting for 78–100% (mean 89%) of radiolarian abundance. The mean total abundance of phaeodarians was 1554 m^{-3} in the Sognefjord complex, 51 m^{-3} in Malangen and 11 m^{-3} in Balsfjord. *Medusetta arcifera* was the most abundant phaeodaria in the Sognefjord complex, accounting for >99% of phaeodarian abundance, but was absent in Malangen and Balsfjord, where *Protocystis tridens* accounted for >96% of phaeodarian abundance. The carbon biomass of *S. zanclea* and *M. arcifera* was 188 and 438 µg C m^{-3}, respectively, which is similar to and 8.6 times higher than, respectively, that of phaeodarians >1 mm in the western North Pacific, suggesting that *M. arcifera* contributes to organic carbon transport in the Sognefjord complex. *Amphimelissa setosa* (Nassellaria, Radiolaria), which was a dominant species in the study area in 1982–83, was absent in the present study in all sampled fjords. This could have been caused by the approximately 2 °C increase in water temperature that has occurred since 1990 and can be taken as evidence of a climate-change-associated local temperature rise linked to the warming of advected Atlantic Water.

Keywords

Zooplankton; biogeochemical cycle; climate change; biodiversity; *Amphimelissa setosa*; local extinction

Correspondence

Takahito Ikenoue, Research Institute for Global Change, Japan Agency for Marine-Earth Science and Technology, 2-15 Natsushima-cho, Yokosuka, Kanagawa 237-0061, Japan. E-mail: ikenouet@jamstec.go.jp

Abbreviations

ESD: equivalent spherical diameter
MALV: marine alveolate
MIS: marine isotope stage
NCBI: National Center for Biotechnology Information (USA)
PCR: polymerase chain reaction
RAS: radiolarian-associated sequence
RHIZ: rhizarian-associated sequence

To access the supplementary material, please visit the article landing page

Introduction

Radiolaria and Phaeodaria are groups of heterotrophic unicellular zooplankton belonging to the supergroup Rhizaria, and both possess skeletons in a wide variety of shapes composed of hydrous amorphous silica ($SiO_2 \cdot nH_2O$, opal; Anderson et al. 2002; Takahashi & Anderson 2002; Adl et al. 2019). The Radiolaria include the following five orders: Collodaria, Nassellaria, Spumellaria, Acantharia and Taxopodia (Suzuki & Not 2015). In this study, we have excluded the Acantharia (which have strontium sulfate skeletons) and Collodaria (which normally do not possess any form of a skeleton) and only consider the Spumellaria and Nassellaria (which typically have a solid skeleton of SiO_2) and the Taxopodia (which only have loose siliceous spicules). Until the early 21st century, Phaeodaria was treated as a group within the Radiolaria, but based on the results of molecular phylogenetic analysis, it is now recognized as a taxon belonging to the phylum Cercozoa (Polet et al. 2004; Yuasa et al. 2006; Nakamura & Suzuki 2015). Radiolaria and Phaeodaria are widely distributed in the global pelagic ocean from the surface to the deep sea (Anderson et al. 2002; Takahashi & Anderson 2002; Lazarus et al. 2021). Radiolaria are

Citation: *Polar Research* 2023, *42*, 9584, http://dx.doi.org/10.33265/polar.v42.9584

generally rare in coastal waters, which have lower salinities than the open ocean, but can be found in areas with salinities above 30, such as in Norwegian fjords (Bjørklund & Swanberg 1987). No freshwater species have been reported to date, but one species is known to inhabit the brackish waters of the La Plata River estuary (Boltovskoy et al. 2003). The importance of radiolarians and phaeodarians in marine material cycling has been noticed in the past (e.g., Takahashi et al. 1983; Bernstein et al. 1990; Takahashi 1991), but this role has received little attention because the current biomass of these two taxa in the ocean is considered to be low. However, radiolarians and phaeodarians do occur with high biomass in some areas (Steinberg et al. 2008; Nakamura et al. 2013; Biard et al. 2016), and their importance to marine ecosystems and material cycles has recently been quantitatively evaluated (Lampitt et al. 2009; Biard et al. 2018; Stukel et al. 2018; Ikenoue, Kimoto et al. 2019; Llopis Monferrer et al. 2020; Ikenoue et al. 2021; Llopis Monferrer et al. 2021).

The abundance distribution of Radiolaria and Phaeodaria in Norwegian fjords was intensively studied in the 1970s and 1980s (e.g., Bjørklund 1974, Bjørklund & Swanberg 1987; Swanberg & Bjørklund 1986, 1987, 1992), and the molecular phylogeny and diversity of their symbiotic algae have been investigated since the 2000s (Yuasa et al. 2006; Dolven et al. 2007; Yuasa et al. 2009; Krabberød et al. 2011; Bråte et al. 2012; Table 1). However, there are no previous reports of the biomass of Radiolaria and Phaeodaria in Norwegian fjords. Therefore, in this study, we deployed plankton nets in Norwegian fjords in September 2016 to determine the abundance distribution of Radiolaria and Phaeodaria and to evaluate the biomass of the principal species, which are usually present throughout the year. Molecular and phylogenetic analysis of symbionts of *Amphimelissa setosa* collected in the Chukchi Sea was also conducted to investigate the ecology of *A. setosa*, which was dominant in Norwegian fjords in 1982–83.

Materials and methods

Study area

Sognefjord, with an average width of about 5 km, is the second-longest fjord in the world, extending 205 km inland from the west coast of Norway and reaching a depth of 1309 m. Along the way, there are many tributary fjords, generally running north–south, created by glacial erosion. This fjord system is connected to the Norwegian Sea via the shallow outer part of Sognefjord, where North Atlantic Water flows in. The inflow of North Atlantic Water takes place not on an annual basis, but on a 5–10-year basis (Hermansen 1974). The water-mass structure of Sognefjord and its tributary fjords (the Sognefjord complex) is characterized by a stratified, low-salinity brackish-water layer and an underlying layer of North Atlantic Water (Swanberg & Bjørklund 1987). This stratification develops because of the large freshwater inputs the fjord complex receives from overland runoff (rivers and snowmelt) and precipitation. In 1982, at a depth of 0–25 m, water temperatures and salinities were in the range of about 7–16 °C and 23–33, respectively, in summer, and 4–11 °C and 23–32, respectively, in winter. At depths of 25–100 m, water temperatures and salinities were about 7 °C and 35, respectively, in summer, and 7–11 °C and 33–34, respectively, in winter.

About 300 km above the Arctic Circle, Balsfjord is a single-basin fjord with a maximum depth of about 195 m. It is 2–7 km wide and runs 57 km south–south-east from

Table 1 Summary of plankton-net tow samples collected in Norwegian fjords during studies of radiolarians and phaeodarians.

Site	Sampling date	Sampling depth (m)	Method	Reference
Korsfjord	Nov. 1969 to May 1971	670–600, 600–500, 500–400, 400–300, 300–200, 200–100, 100–0	Juday net with a closing mechanism and 63-µm mesh	Bjørklund 1974
Hardangerfjord, Sognefjord, Malangen,Balsfjord	Jun./Jul./Dec. 1982, Sep. 1983	1000–500, 500–300, 300–100, 100–25	Juday net with a closing mechanism and 63-µm mesh	Swanberg & Bjørklund 1987
Sogndalsfjord	Oct. 2003	250–25	Nansen plankton net with opening diameter of 30 cm and mesh size of 45 µm	Yuasa et al. 2006; Yuasa et al. 2009
Sogndalsfjord	May/Jun. 2003 and 2004	240–50	Juday net with a closing mechanism and 63-µm mesh	Dolven et al. 2007; Bråte et al. 2012
Sogndalsfjord	Mar./Aug. 2009, Jan. 2010	Unknown	Juday net with a closing mechanism and 63-µm mesh	Krabberød et al. 2011
Sognefjord, Malangen, Balsfjord	Sep. 2016	100–25	Juday net with a closing mechanism and 63-µm mesh	This study

Citation: *Polar Research* 2023, *42*, 9584, http://dx.doi.org/10.33265/polar.v42.9584

the island of Tromsø. During most of the year, its water temperature ranges from 1 to 7 °C and its salinity ranges from 33 to 34 (Eilertsen et al. 1981), making it one of the coldest Norwegian fjords. Water exchange between this fjord and the surrounding coastal waters is greatly restricted by 10–30-m deep sandbar sills located north of the entrance to Balsfjord.

Malangen, west of Balsfjord, is relatively open to the Norwegian Sea. The fjord is 5 km wide and 50 km long and features a much deeper (circa 200 m) sandbar (Falkenhaug et al. 1997). Low-salinity (<33.5) waters are observed from the surface to a depth of 50 m during the summer months, and high temperatures and salinities (mean 6.5 °C and 34.5, respectively) are observed throughout the year in the Malangen basin (Falkenhaug et al. 1997).

Seasonal variations in particulate-matter fluxes are small in the northern Norwegian fjords on account of the smaller scale of river runoff and the greater influence of Atlantic and Norwegian coastal waters compared with the closed coastal systems of the south-western fjords. Particulate matter, phytoplankton and zooplankton fluxes in the coastal zone are mainly influenced by Norwegian coastal waters, where water-mass exchange is faster than in the south-western fjords (Wassmann et al. 1996).

Field sampling

Plankton-tow samples were collected in the fjords during late summer 2016 (Fig. 1). Vertical tows were carried out with a 30-cm Juday net with a mesh size of 63 µm. The

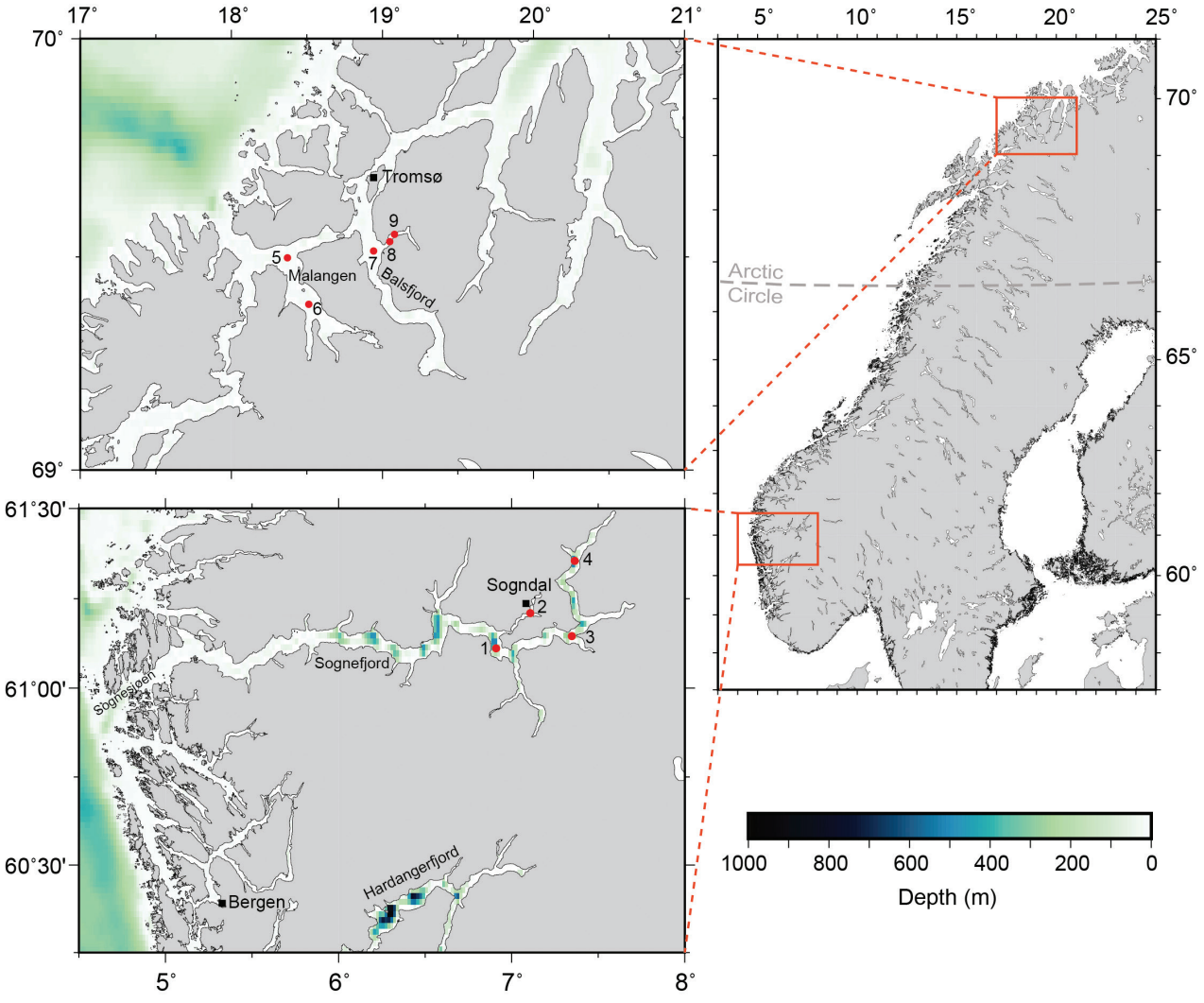

Fig. 1 Maps of the study areas in south-western and northern Norway showing sampling stations (red dots) in the Sognefjord complex, Malangen and Balsfjord.

cod end of the net was weighted and the net lowered slowly to prevent its fishing on descent. The net was closed with a choking mechanism on ascent. On 11 and 13 September 2016, the net was towed at four stations in the Sognefjord complex from depths of 100–25 m from the deck of the RV *Knut* (Industriskjell AS). On 20 and 21 September 2016, the net was towed at five stations in Malangen and Balsfjord from the deck of the RV *Hyas* (UiT The Arctic University of Tromsø). The volume of seawater filtered through the net was calculated by multiplying the distance the net was towed by the opening area of the net. The split samples were fixed with 99.5% ethanol.

For molecular and phylogenetic analysis of symbionts of *A. setosa*, a plankton-tow sample was also collected at station 54 (73.694°N, 162.652°W) in the northern Chukchi Sea using vertical tows from a depth of 150 m to the surface with a North Pacific standard plankton net (62-µm mesh size, open mouth area 0.16 m^2) during the RV *Mirai* Cruise MR13-06 (Ikenoue, Bjørklund et al. 2016; Ikenoue, Bjørklund et al. 2019; Supplementary Fig. S1). The sample was preserved with 99.5% ethanol.

Enumeration of radiolarian and phaeodarian taxa

Plankton samples were split with a Motoda box splitter (Motoda 1959). The split samples were sieved through a stainless-steel screen with mesh size 45 µm. Remains on the screen were filtered through Gelman® membrane filters with a nominal pore size of 0.45 µm. The filtered samples were desalted with distilled water. Slides for light microscope observations were prepared from the filtered samples by using the methods described by Ikenoue et al. (2015). We counted all radiolarian (Spumellaria, Nassellaria and Taxopodia) and phaeodarian specimens observed with an Olympus BX43 transmitted-light microscope on each slide at 200× or 400× magnification. The numbers of counted specimens were converted to standing stocks (i.e., number of specimens m^{-3}).

Estimation of biovolume and elemental content of Rhizaria

To estimate the biovolume of *S. zanclea* and *M. arcifera*, for which particularly high abundances were observed in this study, the ESDs of both were calculated by using the following formula:

$$\mathrm{ESD} = 2\sqrt{\mathrm{Area}/\pi}\,, \tag{1}$$

where ESD (µm) is the ESD and area is the pixel area of the imaged organism. The pixel areas of *S. zanclea* and *M. arcifera* were calculated by using ImageJ, an image processing and analysis programme developed at the US National Institutes of Health (https://imagej.nih.gov/ij/index.html) and images n and q in Fig. 2, respectively. From the ESD, the biovolume (µm³) was calculated by using the following formula:

$$\mathrm{Biovolume} = \frac{4}{3}\pi(0.5\,\mathrm{ESD})^3 \tag{2}$$

Organic C, N, and biogenic Si contents of both species were calculated from their respective biovolumes by using the following equations established by Llopis Monferrer et al. (2020) and Laget et al. (2023):

$$Q_c = 10^{[0.958 \pm 0.025]} V^{[0.455 \pm 0.016]} \tag{3}$$

$$Q_N = 10^{[0.157 \pm 0.026]} V^{[0.477 \pm 0.017]} \tag{4}$$

$$Q_{bSi} = 10^{[-4.05 \pm 0.18]} V^{[0.52 \pm 0.02]}, \tag{5}$$

where Q_C, Q_N, and Q_{bSi} are the organic C (µg-C $cell^{-1}$), N (µg-N $cell^{-1}$), and biogenic Si contents (µg-Si $cell^{-1}$) of each specimen, respectively, and V is the biovolume (mm^3 for Q_C and Q_N, μm^3 for Q_{bSi}).

Molecular and phylogenetic analysis of symbionts of Amphimelissa setosa

The protocol for analysing the symbionts of *A. setosa* was similar to those described in previous studies (Krabberød et al. 2011; Bråte et al. 2012; Ikenoue, Bjørklund et al. 2016). Plankton samples were preserved in 99.5% ethanol and individual *A. setosa* cells were isolated in the laboratory by using capillary isolation. Each cell was cleaned by removing debris with microneedles and then rinsed in three droplets of filtered Milli-Q water. The cleaned cells were transferred to 200-µL PCR tubes for single-cell whole-genome amplification, and 18S PCR with general eukaryotic primers was performed as described by Bråte et al. (2012). The PCR product was Sanger-sequenced on a 3730 Capillary Sequencer. In total, six near-full-length 18S sequences were obtained from five different hosts.

To identify the symbionts, the sequences were blasted against the non-redundant US National Library of Medicine nucleotide database (https://www.ncbi.nlm.nih.gov/nucleotide/) and the PR2 database (version 14.4; Guillou et al. 2013). The top five hits from each search were kept with duplicate hits removed. All sequences were then added to the reference alignment from Ikenoue, Bjørklund et al. (2016). Sequences were aligned with MAFFT version 7.490 (Katoh & Standley 2013) and trimmed with trimAl (Capella-Gutiérrez et al. 2009) by using the settings recommend by EukRef (i.e., -gt 0.3 -st 0.001; Del Campo et al.

Citation: *Polar Research* 2023, *42*, 9584, http://dx.doi.org/10.33265/polar.v42.9584

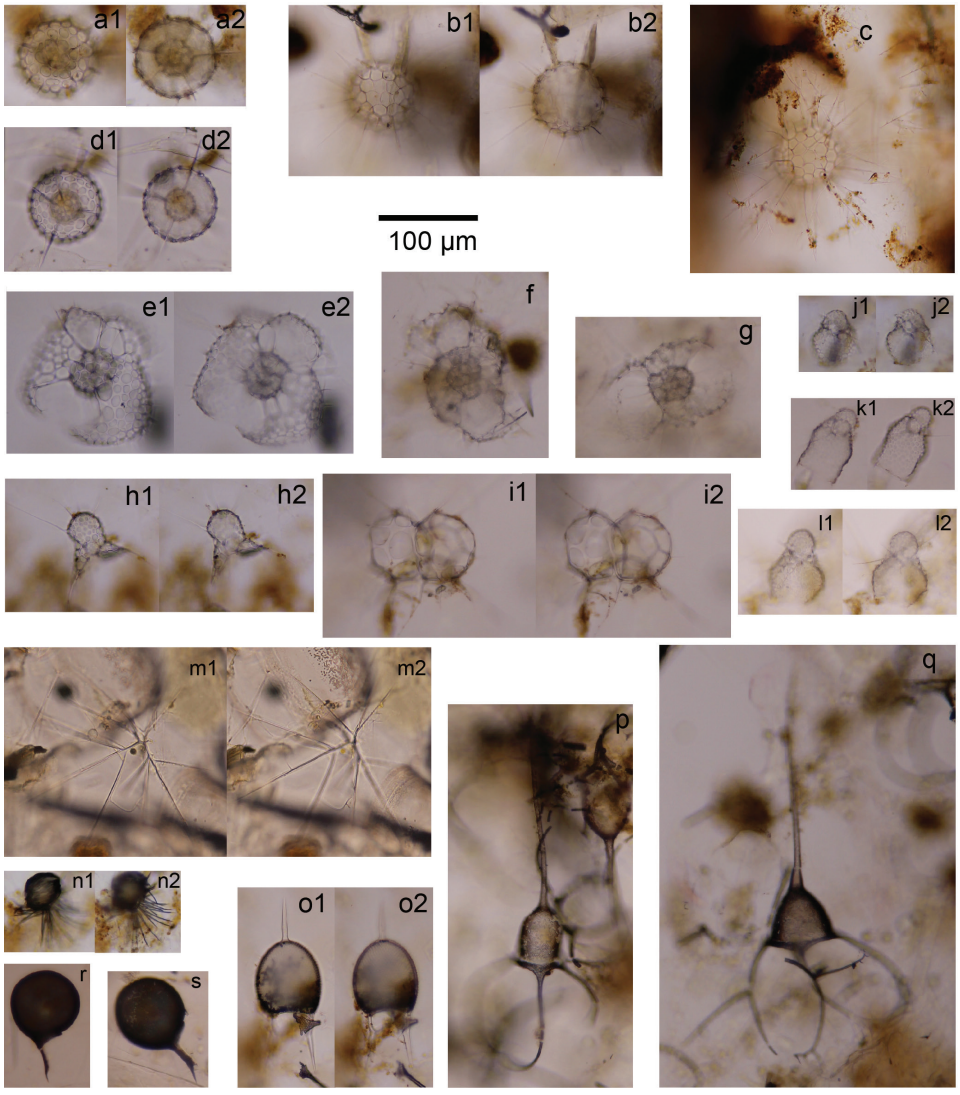

Fig. 2 Light micrographs of radiolarians and phaeodarians identified in south-western and northern Norwegian fjords. (a) *Actinomma leptodermum leptodermum*, (b) *Arachnosphaera dichotoma*, (c) *Cladococcus viminalis*, (d) *Hexaconthium pachydermum*, (e–g) *Phorticium pylonium*, (h) *Arachnocorys umbellifera*, (i) *Ceratospyris hyperborean*, (j–l) *Lithomelissa setosa*, (m) *Plagiacantha arachnoides*, (n) *Sticholonche zancela*, (o) *Challengeron diodon*, (p, q) *Medusetta arcifera*, (r, s) *Protocystis tridens*. The 100 µm scale bar applies to all images.

2018). The final alignment consisted of 231 taxa with 1581 unambiguously aligned characters. Maximum-likelihood analysis with ultrafast bootstrap approximation (UFBoot) and Shimodaira–Hasegawa-like approximate likelihood ratio test (SH-alrt) was performed with IQ-tree2 (Guindon et al. 2010; Hoang et al. 2018; Minh et al. 2020). The tree was visualized with FigTree version 1.4.4 (https://github.com/rambaut/figtree/). Sequences used in this study have been deposited in NCBI GenBank (https://www.ncbi.nlm.nih.gov/) with accession numbers OR469964–OR469969.

Results

Horizontal distribution of radiolarians and phaeodarians

Ten radiolarian species and three phaeodarian species were identified in the plankton-tow samples (Table 2; Fig. 2). The numbers of individuals of each radiolarian and phaeodarian species identified are listed in Table 3. Horizontal distributions of radiolarian and phaeodarian abundance during September 2016 are shown in Fig. 3.

Table 2 List of 10 radiolarian taxa and three phaeodarian taxa encountered in plankton samples from south-western and northern Norwegian fjords.

	Taxa	Taxonomic references
Phylum	Rhizaria, Cavalier-Smith (2002)	
Class	Radiolaria, Müller (1858)	
Sub-class	Polycystina, Ehrenberg (1838); emend. Riedel (1967)	
Order	Spumellaria, Ehrenberg (1876)	
Family	Actinommidae, Haeckel (1862); emend. Riedel (1967)	
	Actinomma leptodermum leptodermum, Jørgensen (1900)	Cortese & Bjørklund 1998a, plate 2, figs. 1–14
	Arachnosphaera dichotoma, Jørgensen (1900)	Dolven et al. 2014, plate 1, figs. 1–4
	Cladococcus viminalis, Haeckel (1862)	Swanberg & Bjørklund 1987, fig. 4J
	Hexaconthium pachydermum, Jørgensen (1900)	Cortese & Bjørklund 1998b
Family	Pyloniidae, Haeckel (1881)	
	Phorticium pylonium, Haeckel (1887)	Bjørklund & Kruglikova 2003, plate 3, figs. 10–12, 14–15
Order	Nassellaria, Ehrenberg (1876)	
Family	Plagiacanthidae, Hertwig (1879)	
	Arachnocorys umbellifera, Haeckel (1862)	Welling 1996, plate 14, figs. 24–27
	Lithomelissa setosa, Jørgensen (1905)	Dolven et al. 2014, plate 6, figs. 10–13
	Plagiacantha arachnoides, Claparède and Lachmann (1858)	Bjørklund et al. 2014, plate 10, fig. 8
Family	Trissocyclidae, Haeckel (1881), emend. Goll (1968)	
	Ceratospyris hyperborea, Jørgensen (1905)	Dolven et al. 2014, plate 4, figs. 11–12
Order	Taxopodida, Fol (1883)	
Family	Sticholonchidae, Hertwig (1877)	
	Sticholonche zanclea, Hertwig (1877)	Krabberød et al. 2011, fig. 1Y
Class	Cercozoa, Cavalier-Smith (1998); emend. Adl et al. (2005)	
Order	Phaeodaria, Haeckel (1879)	
Family	Challengeridae, Murray (1885)	
	Challengeron diodon, Haeckel (1887)	Bjørklund et al. 2014, plate 11, figs. 1–3
	Protocystis tridens, Bjørklund (1976)	Bjørklund et al. 2014, plate 11, fig. 11
Family	Medusettidae, Haeckel (1887)	
	Medusetta arcifera, Jørgensen (1900)	Swanberg & Bjørklund 1987, fig. 4K

Total radiolarian abundance was 35–742 specimens m^{-3} (mean 306) in the Sognefjord complex, 184–1724 specimens m^{-3} (mean 954) in Malangen, and 10–160 specimens m^{-3} (mean 89) in Balsfjord. Total radiolarian abundance was highest at station 6 in Malangen (1724 specimens m^{-3}), followed by station 3 in the Sognefjord complex (742 specimens m^{-3}). In the Sognefjord complex and Malangen, *S. zanclea* was the most abundant radiolarian species, accounting for 78–100% (mean 89%) of the radiolarian abundance. In the Sognefjord complex, *Photicium pylonium* accounted for 22% at station 1, *Actinomma leptodermum leptodermum, Arachnosphaera dichotoma, Hexaconthium pachydermum* and *Arachnocorys umbellifera* together accounted for 20% of radiolarian abundance at station 2. At stations 3–6, species other than *S. zanclea* were scarce. This shows the patchiness of radiolarian distributions in Norwegian fjords, with large differences in species assemblages between adjacent stations. In Balsfjord, *S. zanclea* abundance was low, ranging from 3 to 15% (mean 10%), and *Lithomelissa setosa* and *Plagiacantha arachnoides* accounted for the majority of radiolarian abundance, ranging from 30 to 85% (mean 54%) and 0 to 67% (mean 36%), respectively.

Total phaeodarian abundance was 177–4002 specimens m^{-3} (mean 1554) in the Sognefjord complex, 19–83 specimens m^{-3} (mean 51) in Malangen, and 8–17 specimens m^{-3} (mean 11) in Balsfjord. Total phaeodarian abundance was highest at station 1 in the Sognefjord complex (4002 specimens m^{-3}). *Medusetta arcifera* was the most abundant phaeodarian in the Sognefjord complex, accounting for more than 99% of total phaeodarian abundance, but was not observed in Malangen and Balsfjord, where *P. tridens* accounted for more than 96% of total phaeodarian abundance.

Elemental contents of Sticholonche zanclea *and* Medusetta arcifera

Elemental contents (organic carbon, organic nitrogen and biogenic silica) of *S. zanclea* and *M. arcifera,* which were observed at particularly high abundances in this study, are shown in Table 4. The biomasses of *S. zanclea* and *M. arcifera* in the surface water at each station, calculated from the abundances and elemental contents in Table 4, are shown in Table 5. The highest organic carbon, organic nitrogen, and biogenic silica contents for *S. zanclea* were observed at station 6 and

Citation: *Polar Research* 2023, *42*, 9584, http://dx.doi.org/10.33265/polar.v42.9584

Table 3 Counts of radiolarians and phaeodarians in plankton samples obtained from south-western and northern Norwegian fjords.

Area	Sognefjord complex				Malangen		Balsfjord		
Station	1	2	3	4	5	6	7	8	9
Latitude (°N)	61°6′41.49″	61°12′36.91″	61°8′43.31″	61°21′17.86″	69°29′52.59″	69°23′22.08″	69°30′51.36″	69°32′07.8″	69°33′09.6″
Longitude (°W)	6°54′37.68″	7°6′31.31″	7°20′57.43″	7°21′54.48″	18°22′17.51″	18°30′49.68″	18°56′36.42″	19°02′58.8″	19°04′49.8″E
Sampling date (day/month/year)	13/9/16	11/9/16	13/9/16	13/9/16	20/9/16	20/9/16	21/9/16	21/9/16	21/9/16
Depth interval (m)	25–100	25–100	25–100	25–100	25–100	25–100	25–100	25–100	25–100
Aliquot size[a]	1/8	1/8	1/4	1/4	1/4	1/4	1/4	1/4	1/8
Radiolaria									
Actinomma leptodermum leptodermum	0	2	0	0	2	0	0	0	0
Arachnosphaera dichotoma	0	1	0	0	0	0	0	0	0
Cladococcus viminalis	0	0	1	1	0	0	0	0	0
Hexaconthium pachydermum	0	1	0	1	0	0	0	0	0
Phorticium pylonium	5	0	1	1	4	3	0	2	0
Spumellarida indet.	0	0	0	0	1	2	0	0	0
Arachnocorys umbellifera	0	2	0	0	0	0	0	0	0
Ceratospyris hyperborea	0	0	0	0	1	0	0	0	0
Lithomelissa setosa	0	0	0	0	2	3	11	60	32
Plagiacantha arachnoides	0	0	0	0	4	0	0	51	71
Nassellarida indet.	0	0	0	0	2	0	0	1	0
Sticholonche zanclea	18	24	981	530	228	2276	2	15	3
Total Radiolaria	23	30	983	533	244	2284	13	129	106
Phaeodaria									
Challengeron diodon	0	4	0	0	1	1	0	0	0
Medusetta arcifera	2651	607	1475	234	0	0	0	0	0
Protocystis tridens	0	0	0	0	24	109	11	22	6
Total Phaeodaria	2651	611	1475	234	25	110	11	22	6

[a]The proportion of the entire sample used for radiolarian counts. The numbers given in the body of the table are raw counts of radiolarians in the aliquot used.

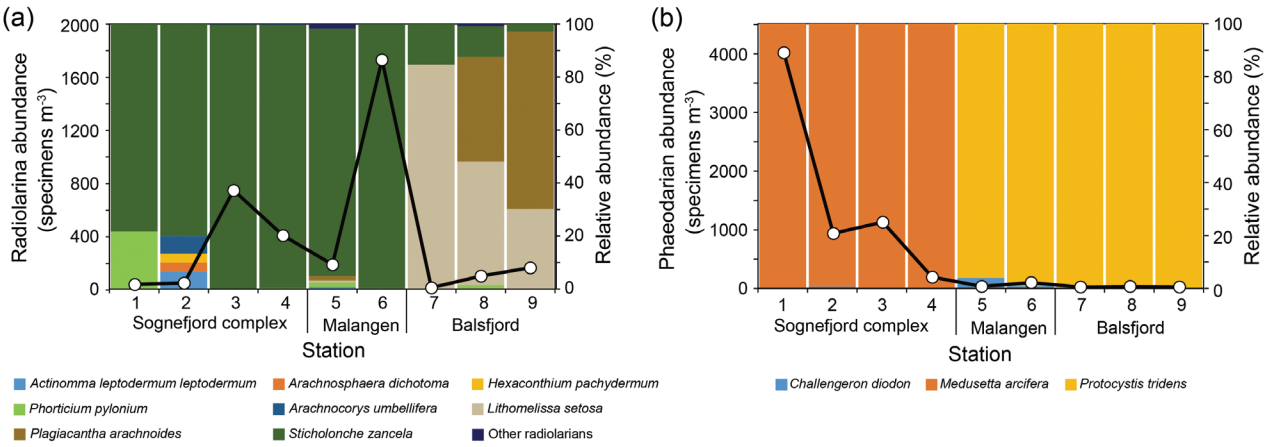

Fig. 3 Abundance (open circles) and species composition (columns) of (a) radiolarians and (b) phaeodarians in surface waters (25–100-m depth) in south-western and northern Norwegian fjords.

Table 4 Summary of organic C, organic N, and biogenic Si contents of *Sticholonche zanclea* and *Medusetta arcifera*. Elemental content and density are expressed as mean ± standard error.

Species	ESD (μm)	Biovolume (mm^3)	Organic C (μg C $cell^{-1}$)	Organic N (μg C $cell^{-1}$)	Biogenic Si (μg Si $cell^{-1}$)
Sticholonche zanclea	49	6.1E-05	0.11 ± 0.02	0.014 ± 0.002	0.027 ± 0.013
Medusetta arcifera	128	1.1E-03	0.41 ± 0.05	0.056 ± 0.007	0.12 ± 0.06

Table 5 Summary of the biomass of *Sticholonche zanclea* and *Medusetta arcifera* in surface waters of south-western and northern Norwegian fjords.

Station	*Sticholonche zanclea* biomass (μg m^{-3})			*Medusetta arcifera* biomass (μg m^{-3})		
	Organic C	Organic N	Biogenic Si	Organic C	Organic N	Biogenic Si
1	3.0 ± 0.5	0.38 ± 0.1	0.74 ± 0.35	1641 ± 202	223 ± 29	495 ± 247
2	4.0 ± 0.7	0.51 ± 0.1	0.99 ± 0.47	376 ± 46	51 ± 7	113 ± 57
3	81 ± 13	10 ± 2	20 ± 10	457 ± 56	62 ± 8	138 ± 69
4	44 ± 7	5.6 ± 1.0	11 ± 5	72 ± 9	10 ± 1	22 ± 11
5	19 ± 3	2.4 ± 0.4	4.7 ± 2.2	0 ± 0	0 ± 0	0 ± 0
6	188 ± 31	24 ± 4	47 ± 22	0 ± 0	0 ± 0	0 ± 0
7	0.17 ± 0.03	0.021 ± 0.004	0.041 ± 0.019	0 ± 0	0 ± 0	0 ± 0
8	1.2 ± 0.2	0.16 ± 0.03	0.31 ± 0.15	0 ± 0	0 ± 0	0 ± 0
9	0.50 ± 0.08	0.063 ± 0.011	0.12 ± 0.06	0 ± 0	0 ± 0	0 ± 0

were 188 ± 31, 24 ± 4 and 47 ± 22 μg m^{-3}, respectively. The highest organic carbon, organic nitrogen and biogenic silica contents for *M. arcifera* were observed at station 1 and were 1641 ± 202, 223 ± 29, and 495 ± 247 μg m^{-3}, respectively.

Symbionts of Amphimelissa setosa

The six symbionts sequenced from *Amphimelissa setosa* in the Chukchi Sea and used for phylogenetic analysis in this study are shown in Table 6. Figure 4 shows a collapsed 18S rDNA phylogeny of MALVs that includes the symbionts from this study, and Supplementary Fig. S2 presents the full phylogenetic tree. All symbionts of *A. setosa* were found to be related to parasitic MALVs, with no photosynthetic representatives.

Of the five sequences from four hosts that grouped within MALV I, three were placed in clades already known to contain symbionts from Radiolaria or

Citation: *Polar Research* 2023, *42*, 9584, http://dx.doi.org/10.33265/polar.v42.9584

Table 6 Symbiont sequences from *Amphimelissa setosa* used for the phylogenetic analysis in this study.

Host sample name	Host species	Symbiont	Associated group
AO02a	*A. setosa*	Marine alveolate	RAS 7
AO02b	*A. setosa*	Marine alveolate	RAS 7
AO06	*A. setosa*	Marine alveolate	RAS 1
AO13	*A. setosa*	Marine alveolate	RHIZ 1
AO46	*A. setosa*	Marine alveolate	RAS 8
AO50	*A. setosa*	Marine alveolate	RAS 6

Phaeodaria, specifically RAS 1, RAS 6, and RHIZ 1 (terminology from Bråte et al. [2012] and Ikenoue, Bjørklund et al. [2016]). Several symbionts from these clades have been observed in samples collected from earlier studies of the Sogndalsfjord (a tributary fjord to the Sognefjord) and the Chukchi Sea (Dolven et al. 2007; Bråte et al. 2012; Ikenoue, Bjørklund et al. 2016). Meanwhile, two sequences from the same host were placed in a clade without previously known radiolarian symbionts, defining the new group RAS 7. This clade is distantly related to RAS 6 from Ikenoue, Bjørklund et al. (2016). The last sequenced symbiont was placed in a small clade between MALV I and MALV II, making up a group (RAS 8) that has not been previously identified. This group was found to be more closely related to symbionts of copepods than to other radiolarian-associated groups.

Discussion

Abundance and biomass of Sticholonche zanclea *and* Medusetta arcifera

Abundances of *S. zanclea* have been reported in the Atlantic Ocean (Emery & Honjo 1979), East China Sea (Tan et al. 1978) and Equatorial Pacific (Takahashi & Ling 1980). In the Equatorial Pacific, *S. zanclea* abundances are highest at depths of 55–110 m near the thermocline and range from 9100 to 25 500 specimens m^{-3} (Takahashi & Ling 1980). In the East China Sea, the maximum abundance reported is 30 000 specimens m^{-3} (Tan et al. 1978). The maximum *S. zanclea* abundance observed in fjords in this study was 1718 specimens m^{-3}, which is an order of magnitude less than those reported in the open ocean. Therefore, *S. zanclea* was considered to prefer open ocean waters to fjord waters. On the other hand, *S. zanclea* was dominant in the inner parts of the Sognefjord complex and Malangen, suggesting that this species is more adapted to the fjord waters than other radiolarians. Since no hydrographic data were obtained in this study, it is not possible to compare water temperatures and salinities at the time the samples were collected. However, because the lowest *S. zanclea* abundances were observed in Balsfjord, one of the coldest Norwegian fjords, it is likely that this species prefers warmer water masses.

Medusetta arcifera has only been reported from western and northern Norwegian fjords and Vestfjord, the water body south of the Lofoten Islands, and has not been observed in the open waters of the Norwegian Sea (Jørgensen 1900, 1905; Swanberg & Bjørklund 1986, 1987). Vestfjord is exposed to the Norwegian Sea and is routinely filled with warm Atlantic Water. This suggests that *M. arcifera* prefers fjord environments. Jørgensen (1905) described *M. arcifera* as probably a temperate type. In a plankton-net survey of western and northern Norwegian fjords conducted in 1982–83, *M. arcifera* was observed only in the Sognefjord complex and not at all in Malangen and Balsfjord (Swanberg & Bjørklund 1987), matching the results obtained in this study and being consistent with the fact that this species was considered a temperate type. In addition, the reported distribution of the species in the Sognefjord complex was similar to that observed in this study, with high abundances observed only at seaward stations, in fjord branches and in polls (Swanberg & Bjørklund 1987). The highest abundances (up to 1142 specimens m^{-3} at depths of 25–100 m) and largest area of distribution were observed in December (winter) 1983, and the species is reported to have been less common in June–July (summer) 1982 and September (late summer) 1983 (Swanberg & Bjørklund 1987). However, 1742 specimens m^{-3} were observed in September (late summer) 2016, exceeding the maximum in winter 1983 (Fig. 3). Since no hydrographic data were obtained in this study, it is not possible to compare water temperatures at the time the samples were collected in December 1983 with those in September 2016. However, since the Sognefjord complex has been experiencing a warming trend in recent years (Reβ 2015), the reason for the increase in abundance of this species during these periods would not be related to seasonal changes in water temperature.

Few articles have reported the carbon contents in seawater of radiolarians and phaeodarians, but carbon contents of 0.0026 µg C m^{-3} and 133 µg C m^{-3} have been reported for Acantharea and Collodaria, respectively, in surface waters around Bermuda (Michaels et al. 1995). In the western North Pacific, a maximum carbon content of 190 µg C m^{-3} has been reported for phaeodarians >1 mm in size at depths of 200–500 m (Ikenoue, Kimoto et al. 2019). These phaeodarians contribute considerably to the transport of organic carbon to the deep sea in the form of sinking particles (Ikenoue, Kimoto et al. 2019). The carbon contents of *S. zanclea* and *M. arcifera* in the present study were 188 µg C m^{-3} and 1641 µg C m^{-3}, respectively,

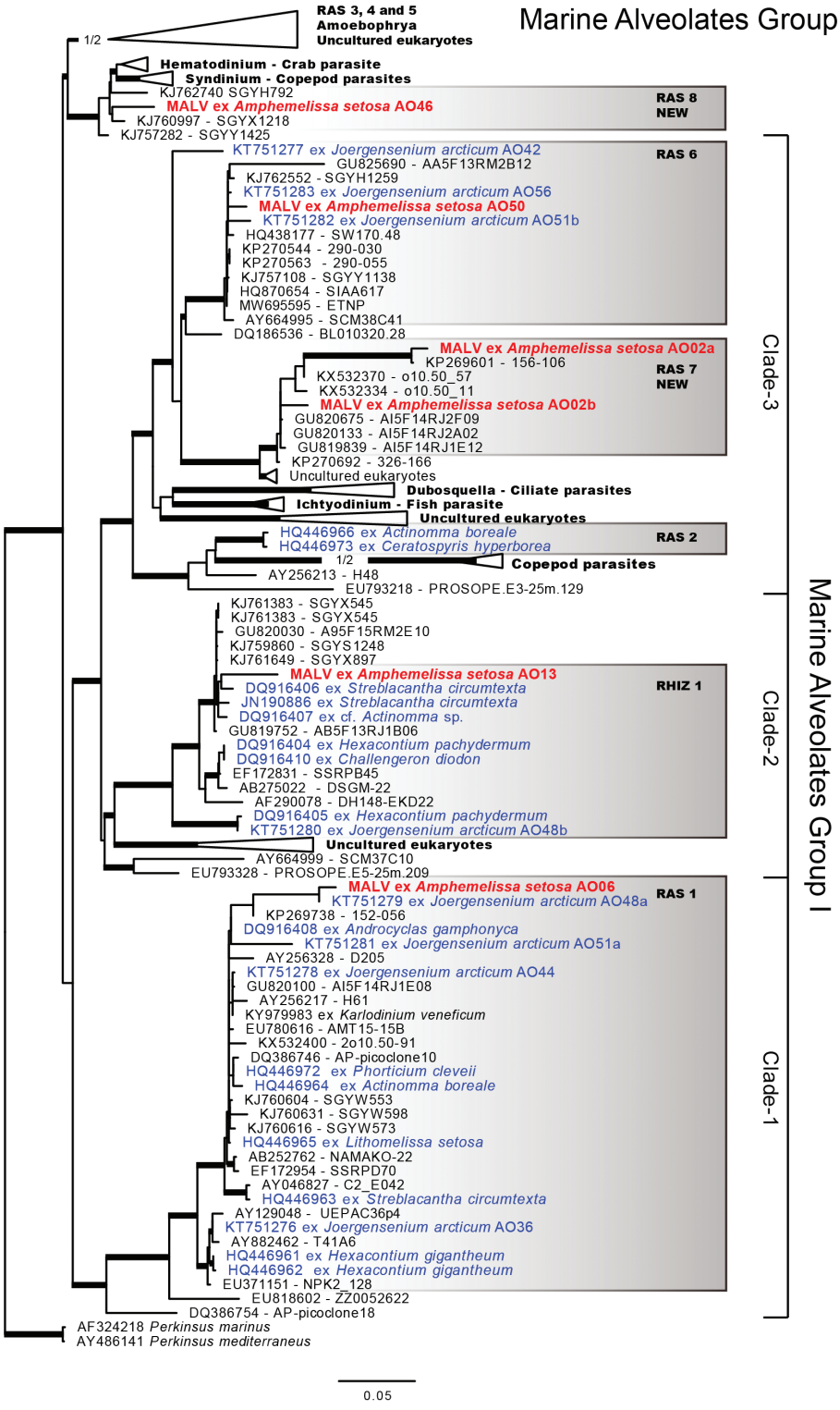

Fig. 4 18S rDNA phylogeny of marine alveolate groups I and II inferred by maximum likelihood analysis in IQ-tree version 2. Thick branches denote strong support (SH-alrt > 80% and UFBoot > 95%). Shaded boxes indicate clades containing MALVs associated with radiolarians and other rhizarian species. Naming schemes follow Bråte et al. (2012) and Ikenoue, Bjørklund et al. (2016): RAS 1–8, RAS clades 1–8; RHIZ 1, RHIZ clade 1. Note that RAS 6 is paraphyletic in this study but was reported to be monophyletic by Ikenoue, Bjørklund et al. (2016). Sequences generated in this study are shown in red, bold type. Other RASs are shown in blue. Because of space limitations, some clades have been collapsed and some branches have been shortened to half their length (marked with "1/2").

Citation: *Polar Research* 2023, *42*, 9584, http://dx.doi.org/10.33265/polar.v42.9584

which are equivalent to and 8.6 times higher than that of >1 mm phaeodarians in the western North Pacific. In the Atlantic, intermittently high concentrations of phaeodarians in the surface layer have been reported to contribute up to 60% of the total organic flux to a depth of 3000 m (Lampitt et al. 2009). Therefore, although the organic carbon transport of *S. zanclea* and *M. arcifera* in the Norwegian fjords is unknown, it is likely that *M. arcifera*—which has a silica skeleton, is a phaeodarian and also occurs in high-abundance patches—contributes strongly to local organic carbon transport in the Sognefjord complex.

Absence of Amphimelissa setosa *in Norwegian fjords during late summer 2016*

Amphimelissa setosa first appeared in the North Pacific 1.5 million years ago and became extinct in the Pacific Ocean about 64 000–85 000 years ago (Matul & Abelmann 2005; Ikenoue, Okazaki et al. 2016; Hernández-Almeida et al. 2020). Migration of *A. setosa* from the Pacific to the Arctic Ocean and Atlantic Ocean occurred during MIS 11 (424–374 thousands of years ago [Bjørklund et al. 2015]), and the modern distribution of *A. setosa* is limited to the Arctic Ocean, high-latitude North Atlantic Ocean, Nordic seas and Norwegian fjords (Bjørklund & Kruglikova 2003). In the northern Chukchi Sea during the summer of 2013 and 2015, *A. setosa* was found at depths of 50–300 m at water temperatures of –1.6 to 1 °C and was not found in the seasonal mixed layer (0–25 m depth), which is characterized by low salinity (<28; Ikenoue et al. 2015; Ikenoue, Bjørklund et al. 2019). The northern Chukchi Sea is almost entirely covered with sea ice from early December to mid-May; the seasonal mixed layer in summer consists of sea-ice melt and river water (Carmack & Wassmann 2006; Nishino et al. 2011). The high abundance of *A. setosa*, especially in waters close to the sea ice margin, was likely caused by predation on microbial communities growing in the seasonal mixed layer and abundant silica supply from melting ice water (Ikenoue, Bjørklund et al. 2019; Hernández-Almeida et al. 2020). None of the symbionts of *A. setosa* reported in the Chukchi Sea are photosynthetic; instead, they are parasitic MALVs (Table 6). The presence of only non-phototrophic symbionts in *A. setosa* suggests that *A. setosa* habitat is not restricted to the photic layer and is consistent with the reported vertical distribution of this species. Since the symbionts are closely related to MALVs previously found associated with radiolarians in both the Sogndalsfjord and the Chukchi Sea, it is likely that the ecology of *A. setosa* in Norwegian fjords is similar to *A. setosa* in the Chukchi Sea.

In the Greenland Sea, *A. setosa* is abundant at depths of 0–300 m in summer near the sea-ice edge at water temperatures below 0 °C (Swanberg & Eide 1992) and does not inhabit low-salinity layers such as the seasonal mixed layer (Ikenoue, Bjørklund et al. 2019). In March 1984, *A. setosa* accounted for 90% of faunal abundance at a location away from the ice edge on the Iceland Plateau at a depth of 3 m and water temperature of 2 °C (Jansen & Bjørklund 1985), which clearly demonstrates the species' preference for shallow and cold waters. *Amphimelissa setosa* also occurs in the Norwegian Sea, where summer water temperatures are relatively high (4–5 °C), but it makes up a much smaller proportion of total radiolarian abundance in this region as compared to the Greenland Sea (Schröder-Ritzrau et al. 2001). The vertical distribution of *A. setosa* in the Norwegian Sea is unknown, but its presence in sediment traps at 500-m depth (Schröder-Ritzrau et al. 2001) indicates that it inhabits waters shallower than 500 m. Based on the current horizontal distribution of *A. setosa*, there is strong evidence that the species prefers cold water masses, especially in the Arctic.

Amphimelissa setosa was observed in the Sognefjord complex as well as in Malangen, Balsfjord and Hardangerfjord during the 1982–83 plankton survey. Especially in the Sognefjord complex, *A. setosa* was the dominant species frequently observed at abundances of thousands of specimens m^{-3} at depths of 25–100 m during summer, late summer and winter (Swanberg & Bjørklund 1987). However, *A. setosa* was entirely absent from the Sognefjord complex, Malangen and Balsfjord during the September 2016 plankton survey in this study (Tables 2, 3). Our study is the only report of radiolarian and phaeodarian community composition in the Sognefjord complex since 1982–83. Plankton-tow samples were also collected in Sogndalsfjord (a tributary fjord to the Sognefjord) from 2003 to 2010 for DNA analysis of radiolarians and phaeodarians (Table 1), and *A. setosa* was also absent from these samples (Yuasa et al. 2006; Dolven et al. 2007; Yuasa et al. 2009; Krabberød et al. 2011; Bråte et al. 2012). All the above-mentioned studies used the same sampling methods except for the plankton tows conducted in October 2003, which used a different mesh size (Table 1).

It is likely that the absence of *A. setosa* in Norwegian fjords since the 2000s is linked to environmental changes within the fjords. Environmental conditions within fjords are affected by the inflow of seawater from the open ocean and freshwater from land as well as by climate change and anthropogenic pollution. North Atlantic Water flows into the Sognefjord, and because Atlantic Water is salty and dense, the Atlantic Water fills the main Sognefjord from bottom to top; this complete water exchange does not occur annually but on a 5–10-year

basis (Hermansen 1974). It is therefore clear that the radiolarian and phaeodarian fauna of the Sognefjord complex represent a local neritic species association (Dolven et al. 2007). In June and December 1982, when *A. setosa* was abundant, water temperatures at depths of 25–100 m in the Sognefjord complex were 7–10 °C, much higher than those in the Chukchi, Greenland and Norwegian seas (Swanberg & Bjørklund 1987). Since the life cycle of *A. setosa* is about three months (Ikenoue et al. 2015), the species, which was dominant from June 1982 to September 1983, clearly adapted to the high temperatures in the Sognefjord complex during this period. The proportion of *A. setosa* relative to other radiolarians decreases as one moves southward from the Arctic Ocean to the Norwegian Sea (Bjørklund & Kruglikova 2003), indicating a preference for cold temperatures, but *A. setosa* is abundant in the warm Sognefjord complex. Swanberg & Bjørklund (1987) described distinct morphotypes of *A. setosa* collected from fjords and the Iceland Plateau. The morphotype found in cold Arctic waters (the present-day habitat of *A. setosa*) is characterized by large, robust skeletons with rounded pores. By contrast, the fjord morphotype is smaller and less silicified and has a more open skeleton with reticulate pores.

Although the biostratigraphy of radiolarians in sediment cores has not been conducted in the Sognefjord complex, radiolarians are known to have first occurred in other Norwegian neritic fjord environments during the late Weichselian glaciation, and *A. setosa* came to dominate the radiolarian fauna during Bølling–Allerød warm periods, with occurrence peaking during the cold Younger Dryas in Korsfjord (Aarseth et al. 1975), Skageraak (Bjørklund 1985) and Andfjord (Bjørklund et al. 2019). During this first phase when the west Norwegian fjords became ice free, the fjords were initially filled with cold Arctic Water, which was gradually replaced by inflowing warm Atlantic Water. The presence of *A. setosa* in Norwegian fjords, both near the end of the last glaciation and during plankton sampling in 1982–83, indicates that *A. setosa* populations in this region were an ice-age relict. As *A. setosa* was also found in very low numbers in plankton collected in 1969–71 from Korsfjord (Bjørklund 1974), relict populations could have survived in at least some Norwegian fjords, such as in the Sognefjord complex.

The sills of fjords are important for water circulation and may have facilitated the development of special ecological niches where *A. setosa* settled, thrived, developed a distinct skeletal morphotype and adapted to much higher temperatures than those that were prevalent when it was first introduced to the fjords at the end of the last glaciation. Korsfjord is more exposed to the open ocean than the Sognefjord complex, but in the remote Sognefjord, *A. setosa* might have survived longer, adapted and become an ice-age relict. Ice formation in the inner part of Sognefjord in winter and the influx of glacial meltwater from land in summer would have created a water mass similar to the low-salinity surface layer of the Chukchi Sea (0–25 m). Therefore, the food and silica supply from the low-salinity surface water-mass in the inner part of Sognefjord might have created a viable environment for *A. setosa*. However, at Sognesjøen, a strait at the entrance of Sognefjord (Fig. 1), surface water temperature has increased markedly since the 1990s (Fig. 5). Water temperatures at Sognesjøen have been monitored at depths of 10 and 200 m from 1940 to 2022, and a marked summer water temperature increase since 1990 has been observed at 10 m (Fig. 5a). During 2000–09, the mean temperature at 10 m was 14.1 °C, an increase of about 1.6 °C compared with the period 1940–89. During 2010–19, mean water temperatures increased an additional 0.4 °C, meaning the temperatures were about 2.0 °C above the mean for the period 1940–89 (Fig. 5a). Prior to 1990, the 10-year mean water temperature at 200-m depth varied only slightly from 7.6 to 7.9 °C (Fig. 5b). However, after 1990, the average temperature for the period 2000–09 increased to 8.4 °C. The increase in temperature compared with the period 1940–89 was about 0.7 °C (Fig.5b).

Amphimelissa setosa has not been observed in any Norwegian fjord since the early 2000s. We are now of the opinion that *A. setosa* probably reached its upper limit of ecological tolerance, and we point to the surface water temperature increase (an increase of 1.6 °C since the 1990s) as the most probable factor explaining its disappearance. The fate of new *A. setosa* individuals entering the Sognefjord complex from Atlantic waters is uncertain, but it may take time on a geological scale for this species, which is adapted to cold waters, to adapt to the high present-day temperatures of the Sognefjord complex. We therefore assume that *A. setosa* is now extinct in Norwegian neritic environments, and we suggest that this is evidence of the impact of global warming.

Conclusion

Our results suggest that *M. arcifera* and *S. zanclea* contribute to biogeochemical cycling in the Sognefjord complex and Malangen, respectively. Radiolarian faunal composition in 2016 differed considerably from that in 1982–83, and *A. setosa*, a key species in 1982–83, was not observed at all in 2016. It is not certain whether *A. setosa* has become extinct in the Norwegian fjords, but it may have become threatened with extinction due to a remarkable increase in water temperatures in Norwegian fjords since 1990. Future studies on the genetic differences between *A. setosa* in the Sognefjord complex and in the Arctic

Citation: *Polar Research* 2023, *42*, 9584, http://dx.doi.org/10.33265/polar.v42.9584

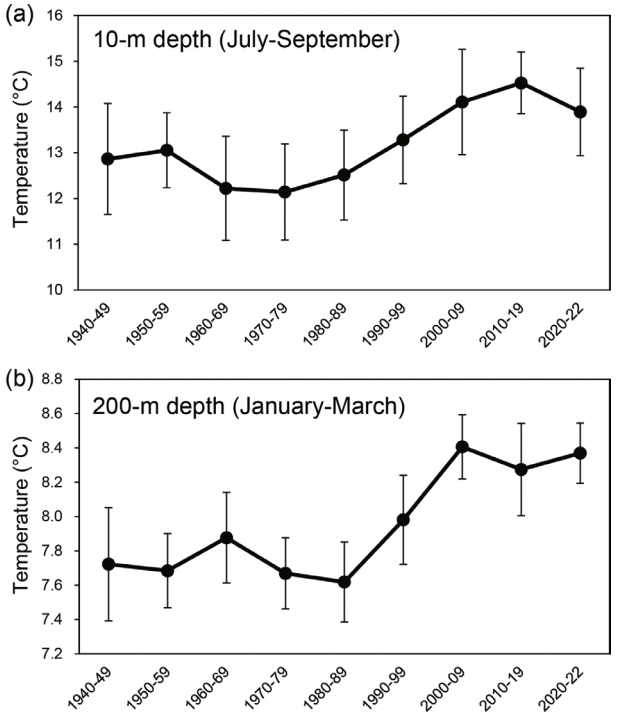

Fig. 5 Decadal mean temperatures (1940–2022) at Sognesjøen (a) in the surface layer (10-m depth) during July–September and (b) at 200-m depth in January–March. The error bars indicate the standard deviations of the decadal mean temperatures. Data from the fixed hydrographical station at Sognesjøen are provided by the Institute of Marine Research, Norway (Institute of Marine Research 2023).

Ocean, as well as high-resolution biostratigraphy of *A. setosa* in sediment cores from the previous 2000 years, could provide more detailed information on the impacts of environmental changes in the fjords due to global warming.

Acknowledgements

The authors would like to thank Peter and Kjartan Hovgaard of Industriskjell AS (Sogndal, Norway) for their assistance during plankton sampling in the Sognefjord complex. They also thank Sigrid Øygarden for technical support in the laboratory and Kunuk Lennert, Ivan Tatone, Valentina Lanci and Frode Gerhardsen of UiT The Arctic University of Tromsø (Tromsø, Norway) for assistance during plankton sampling in Malangen and Balsfjord. They are also grateful to the captain, officers and crews of the RV *Mirai* and also acknowledge O.R. Anderson (Lamont-Doherty Earth Observatory of Columbia University, Palisades, NY, USA) and Vikki Lowe (School of Earth and Environmental Sciences, The University of Queensland, Brisbane, QLD, Australia) for their critical reviews, with many helpful comments and suggestions.

Disclosure statement

The authors report no conflict of interest.

Funding

This study was supported by Grants-in-Aid for Scientific Research from the Japan Society for the Promotion of Science (grant nos. 26740006 and 23K11414) to TI, and by the Arctic Challenge for Sustainability II (grant no. JPMXD1420318865), funded by the Ministry of Education, Culture, Sports, Science and Technology, Japan.

References

Aarseth I., Bjerkli K., Björklund K.R., Böe D., Holm J.P., Lorentzen-Styr T.J., Myhre L.A., Ugland E.S. & Thiede J. 1975. Late quaternary sediments from Korsfjorden, western Norway. *Sarsia 58*, 43–66, doi: 10.1080/00364827.1975.10411278.

Adl S.M., Bass D., Lane C.E., Lukeš J., Schoch C.L., Smirnov A., Agatha S., Berney C., Brown M.W., Burki F., Cárdenas P., Čepička I., Chistyakova L., Del Campo J., Dunthorn M., Edvardsen B., Eglit Y., Guillou L., Hampl V., Heiss A.A., Hoppenrath M., James T.Y., Karnkowska A., Karpov S., Kim E., Kolisko M., Kudryavtsev A., Lahr D.J.G., Lara E., Le Gall L., Lynn D.H., Mann D.G., Massana R., Mitchell E.A.D., Morrow C., Park J.S., Pawlowski J.W., Powell M.J., Richter D.J., Rueckert S., Shadwick L., Shimano S., Spiegel F.W., Torruella G., Youssef N., Zlatogursky V. & Zhang Q. 2019. Revisions to the classification, nomenclature, and diversity of eukaryotes. *Journal of Eukaryotic Microbiology 66*, 4–119, doi: 10.1111/jeu.12691.

Adl S.M., Simpson G.B., Farmer M.A., Andersen R.A., Anderson O.R., Barta J.R., Bowser S.S., Brugerolle G., Fensome R.A., Fredericq S., James T.Y., Karpov S., Kugrens P., Krug J., Lane C.E., Lewis L.A., Lodge J., Lynn D.H., Mann D.G., Mccourt R.M., Mendoza L., Moestrup Ø., Mozley-Standridge S.E., Nerad, T.A., Shearer C.A., Smirnov A.V., Spiegel F.W. & Taylor M.F.J.R. 2005. The new higher level classification of eukaryotes with emphasis on the taxonomy of protists. *Journal of Eukaryotic Microbiology 52*, 399–451, doi: 10.1111/j.1550-7408.2005.00053.x.

Anderson O.R., Nigrini C., Boltovskoy D., Takahashi K. & Swanberg N.R., 2002. Class Polycystina. In J.J. Lee et al. (eds.): *The second illustrated guide to the protozoa*. Pp. 994–1022. Lawrence, KS: Society of Protozoologists.

Bernstein R.E., Betzer P.R. & Takahashi K. 1990. Radiolarians from the western North Pacific Ocean: a latitudinal study of their distributions and fluxes. *Deep-Sea Research Part A 37*, 1677–1696, doi: 10.1016/0198-0149(90)90071-3.

Biard T., Krause J.W., Stukel M.R. & Ohman M.D. 2018. The significance of giant Phaeodarians (Rhizaria) to biogenic silica export in the California Current ecosystem. *Global Biogeochemical Cycles 32*, 987–1004, doi: 10.1029/2018GB005877.

Biard T., Stemmann L., Picheral M., Mayot N., Vandromme P., Hauss H., Gorsky G., Guidi L., Kiko R. & Not F. 2016. In situ imaging reveals the biomass of giant protists in the global ocean. *Nature 532*, 504–507, doi: 10.1038/nature17652.

Bjørklund K.R. 1974. The seasonal occurrence and depth zonation of radiolarians in Korsfjorden, western Norway. *Sarsia 56*, 13–42, doi: 10.1080/00364827.1974.10411259.

Bjørklund K.R. 1976. Radiolaria from the Norwegian Sea, Leg 38 of the Deep Sea Drilling Project. *Initial Reports of the Deep Sea Drilling Project 38*, 1101–1168, doi: 10.2973/dsdp.proc.38.131.1976

Bjørklund K.R. 1985. Upper Weichselian–Holocene radiolarian stratigraphy in the Skagerrak (NE North Sea). *Norsk Geologisk Tidsskrift 65*, 103–106.

Bjørklund K.R., Hatakeda K., Kruglikova S.B. & Matul A.G. 2015. *Amphimelissa setosa* (Cleve) (Polycystina, Nassellaria)—a stratigraphic and paleoecological marker of migrating polar environments in the Northern Hemisphere during the quaternary. *Stratigraphy 12*, 23–37.

Bjørklund K.R., Itaki T. & Dolven J.K. 2014. Per Theodor Cleve: a short résumé and his radiolarian results from the Swedish Expedition to Spitsbergen in 1898. *Journal of Micropalaeontology 33*, 59–93, doi: 10.1144/jmpaleo2012-024.

Bjørklund K.R. & Kruglikova S.B. 2003. Polycystine radiolarians in surface sediments in the Arctic Ocean basins and marginal seas. *Marine Micropaleontology 49*, 231–273, doi: 10.1016/S0377-8398(03)00036-7.

Bjørklund K.R., Kruglikova S.B. & Hammer Ø. 2019. The radiolarian fauna during the Younger Dryas–Holocene transition in Andfjorden, northern Norway. *Polar Research 38*, article no. 3444, doi: 10.33265/polar.v38.3444.

Bjørklund K.R. & Swanberg N.R. 1987. The distribution of two morphotypes of the radiolarian *Amphimelissa setosa* Cleve (Nassellarida): a result of environmental variability? *Sarsia 72*, 245–254, doi: 10.1080/00364827.1987.10419721.

Boltovskoy D., Kogan M., Alder V.A. & Mianzan H. 2003. First record of a brackish radiolarian (Polycystina): *Lophophaena rioplatensis* n. sp. in the Río de la Plata estuary. *Journal of Plankton Research 25*, 1551–1559, doi: 10.1093/plankt/fbg107.

Bråte J., Krabberød A.K., Dolven J.K., Ose R.F., Kristensen T., Bjørklund K.R. & Shalchian-Tabrizi K. 2012. Radiolaria associated with large diversity of marine alveolates. *Protist 163*, 767–777, doi: 10.1016/j.protis.2012.04.004.

Capella-Gutiérrez S., Silla-Martínez J.M. & Gabaldón T. 2009. trimAl: a tool for automated alignment trimming in large-scale phylogenetic analyses. *Bioinformatics 25*, 1972–1973, doi: 10.1093/bioinformatics/btp348.

Carmack E. & Wassmann P. 2006. Food webs and physical–biological coupling on pan-Arctic shelves: unifying concept and comprehensive perspectives. *Progress in Oceanography 71*, 446–477, doi: 10.1016/j.pocean.2006.10.004.

Cavalier-Smith T. 1998. A revised six-kingdom system of life. *Biological Reviews 73*, 203–266, doi: 10.1017/S0006323198005167.

Cavalier-Smith T. 2002. The phagotrophic origin of eukaryotes and phylogenetic classification of protozoa. *International Journal of Systematic and Evolutionary Microbiology 52*, 297–354, doi: 10.1099/00207713-52-2-297.

Claparède E. & Lachmann J. 1858. *Études sur les infusoires et les Rhizopodes. (Studies of infusoria and rhizopods.) Mémoires de l'Institut National Genevois 6*, 261–482.

Cortese G. & Bjørklund K.R. 1998a. The taxonomy of boreal Atlantic Ocean Actinommida (Radiolaria). *Micropaleontology 44*, 149–160, doi: 10.2307/1486067.

Cortese G. & Bjørklund K.R. 1998b. Morphometry and taxonomy of *Hexacontium* species from western Norwegian fjords. *Micropaleontology 44*, 161–172, doi: 10.2307/1486068.

Del Campo J., Kolisko M., Boscaro V., Santoferrara L.F., Nenarokov S., Massana R., Guillou L., Simpson A., Berney C., de Vargas C., Brown M.W., Keeling P.J. & Wegener Parfrey L. 2018. EukRef: phylogenetic curation of ribosomal RNA to enhance understanding of eukaryotic diversity and distribution. *PLoS Biology 16*, e2005849, doi: 10.1371/journal.pbio.2005849.

Dolven J.K., Bjørklund K.R. & Itaki T. 2014. Jørgensen's polycystine radiolarian slide collection and new species. *Journal of Micropalaeontology 33*, 21–58, doi: 10.1144/jmpaleo2012-027.

Dolven J.K., Lindqvist C., Albert V.A., Bjørklund K.R., Yuasa T., Takahashi O. & Mayama S. 2007. Molecular diversity of alveolates associated with neritic North Atlantic radiolarians. *Protist 158*, 65–76, doi: 10.1016/j.protis.2006.07.004.

Ehrenberg C.G. 1838. Über die Bildung der Kreidefelsen und des Kreidemergels durch unsichtbare Organismen. (On the formation of chalk cliffs and chalk marl by invisible organisms.) *Abhandlungen der Königlichen Akademie der Wissenschaften zu Berlin 1838*, 59–147.

Ehrenberg C.G. 1876. Fortsetzung der mikrogeologischen Studien als Gesammt-Uebersicht der mikroskopischen Paläontologie gleichartig analysirter Gebirgsarten der Erde, mit specieller Rücksicht auf den Polycystinen-Mergel von Barbados. (Continuation of the microgeological studies as a general overview of the microscopic palaeontology of the Earth's rock types analysed in the same way, with special regard to the polycystine marl of Barbados.) *Abhandlungen der Königliche Akademie der Wissenschaften zu Berlin 1875*, 1–225.

Eilertsen H.C., Falk-Petersen S., Hopkins C.C.E. & Tande K. 1981. Ecological investigations on the plankton community of Balsfjorden, northern Norway: program for the project, study area, topography, and physical environment. *Sarsia 66*, 25–34, doi: 10.1080/00364827.1981.10414517.

Emery K.O. & Honjo S. 1979. Surface suspended matter off western Africa: relations of organic matter, skeletal debris and detrital minerals. *Sedimentology 26*, 775–794, doi: 10.1111/j.1365-3091.1979.tb00972.x.

Falkenhaug T., Tande K. & Timonin A. 1997. Spatio-temporal patterns in the copepod community in Malangen, northern Norway. *Journal of Plankton Research 19*, 449–468, doi: 10.1093/plankt/19.4.449.

Fol H. 1883. Sur le *Sticholonche zanclea* et un nouvel ordre de Rhizopodes. (On *Sticholonchea zanclea* and a new order of Rhizopoda.) *Mémoires de l'Institut National Genevois 15*, 1–35.

Goll R.M. 1968. Classification and phylogeny of Cenozoic Trissocyclidae (Radiolaria) in the Pacific and Caribbean basins. *Part I. Journal of Paleontology 42*, 1409–1432.

Guillou L., Bachar D., Audic S., Bass D., Berney C., Bittner L., Boutte C., Burgaud G., de Vargas C. & Decelle J. 2013. The Protist Ribosomal Reference Database (PR2): a catalog of unicellular eukaryote small sub-unit rRNA sequences with curated taxonomy. *Nucleic Acids Research 41*, D597–D604, doi: 10.1093/nar/gks1160.

Guindon S., Dufayard J.F., Lefort V., Anisimova M., Hordijk W. & Gascuel O. 2010. New algorithms and methods to estimate maximum-likelihood phylogenies: assessing the performance of PhyML 3.0. *Systematic Biology 59*, 307–321, doi: 10.1093/sysbio/syq010.

Haeckel E. 1862. *Die Radiolarien (Rhizopoda Radiaria). Eine Monographie. (The radiolarians [Rhizopoda radiaria].)* Berlin: Reimer.

Haeckel E. 1879. Über die Phaeodarien, eine neue Gruppe kieselschaliger mariner Rhizopoden. (On the Phaeodaria, a new group of siliceous marine rhizopods.) *Jenaische Zeitschrift für Naturwissenschaft 14*, 151–157.

Haeckel E. 1881. Prodromus Systematis Radiolarium, Entwurf eines Radiolarien-Systems auf Grund von Studien der *Challenger*-Radiolarien. (Preliminary publication on the Radiolaria, based on studies of the *Challenger* radiolarian species.) *Jenaische Zeitschrift für Naturwissenschaft 15*, 418–472.

Haeckel E. 1887. *Report on the Radiolaria collected by the H.M.S. Challenger during the years 1873–1876. Report on the Scientific Results of the Voyage of H.M.S. Challenger during the years 1873–76. Zoology. Vol. 18.* London: Her Majesty's Stationary Office.

Hermansen O.H. 1974. *Sognefjordens hydrografi og vannutveksling. (Sognefjord's hydrography and water exchange.)* MSc thesis, University of Bergen.

Hernández-Almeida I., Björklund K.R., Diz P., Kruglikova S., Ikenoue T., Matul A., Saavedra-Pellitero M. & Swanberg N. 2020. Life on the ice-edge: paleoenvironmental significance of the radiolarian species *Amphimelissa setosa* in the Northern Hemisphere. *Quaternary Science Reviews 248*, article no. 106565, doi: 10.1016/j.quascirev.2020.106565.

Hertwig R. 1877. Studien uber Rhizopoden. (Studies of Rhizopoda.) *Jenaische Zeitschrift für Naturwissenschaft 11*, 324–348.

Hertwig R. 1879. Der organismus der Radiolarien. (The organisms of the radiolarians.) *Jenaische Denkschriften 2*, 129–277.

Hoang D.T., Chernomor O., Von Haeseler A., Minh B.Q. & Vinh L.S. 2018. UFBoot2: improving the ultrafast bootstrap approximation. *Molecular Biology and Evolution 35*, 518–522, doi: 10.1093/molbev/msx281.

Ikenoue T., Bjørklund K.R., Dumitrica P., Krabberød A.K., Kimoto K., Matsuno K. & Harada N. 2016. Two new living Entactinaria (Radiolaria) species from the Arctic province: *Joergensenium arcticum* n. sp. and *Joergensenium clevei* n. sp. *Marine Micropaleontology 124*, 75–94, doi: 10.1016/j.marmicro.2016.02.003.

Ikenoue T., Bjørklund K.R., Fujiwara A., Uchimiya M., Kimoto K., Harada N. & Nishino S. 2019. Horizontal and vertical distribution of polycystine radiolarians in the western Arctic Ocean during the late summers of 2013 and 2015. *Polar Biology 42*, 285–305, doi: 10.1007/s00300-018-2421-3.

Ikenoue T., Bjørklund K.R., Kruglikova S.B., Onodera J., Kimoto K. & Harada N. 2015. Flux variations and vertical distributions of siliceous Rhizaria (Radiolaria and Phaeodaria) in the western Arctic Ocean: indices of environmental changes. *Biogeosciences 12*, 2019–2046, doi: 10.5194/bg-12-2019-2015.

Ikenoue T., Kimoto K., Nakamura Y., Bjørklund K.R., Kuramoto N., Ueki M., Ota Y., Onodera J., Harada N., Honda M.C., Sato M., Watanabe E., Itoh M., Nishino S. & Kikuchi T. 2021. New evaluation of species-specific biogenic silica flux of radiolarians (Rhizaria) in the western Arctic Ocean using microfocus x-ray computed tomography. *Limnology Oceanography 66*, 3901–3915, doi: 10.1002/lno.11928.

Ikenoue T., Kimoto K., Okazaki Y., Sato M., Honda M.C., Takahashi K., Harada N. & Fujiki T. 2019. Phaeodaria: an important carrier of particulate organic carbon in the mesopelagic twilight zone of the North Pacific Ocean. *Global Biogeochemical Cycles 33*, 1146–1160, doi: 10.1029/2019GB006258.

Ikenoue T., Okazaki Y., Takahashi K. & Sakamoto T. 2016. Bering Sea radiolarian biostratigraphy and paleoceanography at IODP Site U1341 during the last four million years. *Deep-Sea Research Part II 125*, 38–55, doi: 10.1016/j.dsr2.2015.03.004.

Institute of Marine Research 2023. Faste hydrografiske stasjoner. (Fixed hydrographical stations.) Accessed on the internet at http://www.imr.no/forskning/forskningsdata/stasjoner/index.html on 11 Apil 2023.

Jansen E. & Bjørklund K.R. 1985. Surface ocean circulation in the Norwegian Sea 15,000 BP to present. *Boreas 14*, 243–257, doi: 10.1111/j.1502-3885.1985.tb00729.x.

Jørgensen E. 1900. Protophyten und Protozöen im Plankton aus der norwegischen Westküste. (Protophytes and protozoa in plankton from the west coast of Norway.) *Bergens Museums Aarbog 1899 6*, 51–112.

Jørgensen E. 1905. The Protist plankton and the diatoms in bottom samples. Plates VIII–XVIII. *Bergens Museums Skrifter 1*, 49–151.

Katoh K. & Standley D.M. 2013. MAFFT multiple sequence alignment software version 7: improvements in performance and usability. *Molecular Biology and Evolution 30*, 772–780, doi: 10.1093/molbev/mst010.

Krabberød A.K., Bråte J., Dolven J.K., Ose R.F., Klaveness D., Kristensen T., Bjørklund K.R. & Shalchian-Tabrizi K. 2011. Radiolaria divided into Polycystina and Spasmaria in combined 18S and 28Sr DNA phylogeny. *PLoS One 6*, e23526, doi: 10.1371/journal.pone.0023526.

Laget M., Llopis Monferrer N., Maguer J.F., Leynaert A. & Biard T. 2023. Elemental content allometries and silicon uptake rates of planktonic Rhizaria: insights into their ecology and role in biogeochemical cycles. *Limnology and Oceanography 68*, 439–454, doi: 10.1002/lno.12284.

Lampitt R.S., Salter I. & Johns D. 2009. Radiolaria: major exporters of organic carbon to the deep ocean. *Global Biogeochemical Cycles 23*, GB1010, doi: 10.1029/2008GB003221.

Lazarus D., Suzuki N., Ishitani Y. & Takahashi K. 2021. *Paleobiology of the polycystine Radiolaria*. Chichester, UK: John Wiley and Sons.

Llopis Monferrer N., Boltovskoy D., Tréguer P., Sandin M.M., Not F. & Leynaert A. 2020. Estimating biogenic silica production of Rhizaria in the global ocean. *Global Biogeochemical Cycles 34*, e2019GB006286, doi: 10.1029/2019GB006286.

Llopis Monferrer N., Leynaert A., Tréguer P., Gutiérrez-Rodríguez A., Moriceau B., Gallinari M., Latasa M., L'Helguen S., Maguer J.-F., Safi K., Pinkerton M.H. & Not F. 2021. Role of small Rhizaria and diatoms in the pelagic silica production of the Southern Ocean. *Limnology and Oceanography 66*, 2187–2202, doi: 10.1002/lno.11743.

Matul A.G. & Abelmann A. 2005. Pleistocene and Holocene distribution of the Radiolarian *Amphimelissa setosa* Cleve in the North Pacific and North Atlantic: evidence for water mass movement. *Deep-Sea Research Part II 52*, 2351–2364, doi: 10.1016/j.dsr2.2005.07.008.

Michaels A.F., Caron D.A., Swanberg N.R., Howse F.A. & Michaels C.M. 1995. Planktonic sarcodines (Acantharia, Radiolaria, Foraminifera) in surface waters near Bermuda: abundance, biomass and vertical flux. *Journal of Plankton Research 17*, 131–163, doi: 10.1093/plankt/17.1.131.

Minh B.Q., Schmidt H.A., Chernomor O., Schrempf D., Woodhams M.D., von Haeseler A. & Lanfear R. 2020. IQ-TREE 2: new models and efficient methods for phylogenetic inference in the genomic era. *Molecular Biology and Evolution 37*, 1530–1534, doi: 10.1093/molbev/msaa015.

Motoda S. 1959. Devices of simple plankton apparatus. *Memoirs of the Faculty of Fisheries Hokkaido University 7*, 73–94.

Müller J. 1858. Über die Thalassicollen, Polycystinen und Acanthometren des Mittelmeeres. (About the Thalassicolla, Polycystines and Acanthometra of the Mediterranean Sea.) *Abhandlungen der Königliche Akademie der Wissenschaften zu Berlin 1858*, 1–62.

Murray T.H. 1885. The Radiolaria. In C.W. Thomson & T.H. Murray (eds.): *Report on the scientific results of the voyage of the H.M.S. Challenger during the years 1873–76. Narrative. Vol. 1. First Part.* Pp. 219–227. London: Her Majesty's Stationary Office.

Nakamura Y., Imai I., Yamaguchi A., Tuji A. & Suzuki N. 2013. *Aulographis japonica* sp. nov. (Phaeodaria, Aulacanthida, Aulacanthidae), an abundant zooplankton in the deep sea of the Sea of Japan. *Plankton and Benthos Research 8*, 107–115, doi: 10.3800/pbr.8.107.

Nakamura Y. & Suzuki N. 2015. Phaeodaria: diverse marine cercozoans of world-wide distribution. In S. Ohtsuka et al. (eds.): *Marine protists*. Pp. 223–249. Tokyo, Japan: Springer.

Nishino S., Kikuchi T., Yamamoto-Kawai M., Kawaguchi Y., Hirawake T. & Itoh M. 2011. Enhancement/reduction of biological pump depends on ocean circulation in the sea-ice reduction regions of the Arctic Ocean. *Journal of Oceanography 67*, 305–314, doi: 10.1007/s10872-011-0030-7.

Polet S., Berney C., Fahrni J. & Pawlowski J. 2004. Small subunit ribosomal RNA gene sequences of Phaeodarea challenge the monophyly of Haeckel's Radiolaria. *Protist 155*, 53–63, doi: 10.1078/1434461000164.

Reβ T. 2015. *Some hydrographical changes in the Sognefjord and its tributaries, the Sogndalsfjord and the Barsnesfjord (Western Norway), the last century.* Bachelor's thesis, Sogn og Fjordane University College, Norway.

Riedel W.R. 1967. Subclass radiolaria. In W.B. Harland et al. (eds.): *The fossil record: a symposium with documentation.* Pp. 291–298. London: Geological Society of London.

Schröder-Ritzrau A., Andruleit H., Jensen S., Samtleben C., Schäfer P., Matthiessen J., Hass, H.C., Kohly A. & Thiede J. 2001. Distribution, export and alteration of fossilizable plankton in the Nordic Seas. In P. Schäfer et al. (eds.): *The northern North Atlantic: a changing environment*. Pp. 81–104. Berlin: Springer.

Steinberg D.K., Cope J.S., Wilson S.E. & Kobari T. 2008. A comparison of mesopelagic mesozooplankton community structure in the subtropical and Subarctic North Pacific Ocean. *Deep-Sea Research Part II 55*, 1615–1635, doi: 10.1016/j.dsr2.2008.04.025.

Stukel M.R., Biard T., Krause J. & Ohman M.D. 2018. Large Phaeodaria in the twilight zone: their role in the carbon cycle. *Limnology and Oceanography 63*, 2579–2594, doi: 10.1002/lno.10961.

Suzuki N. & Not F. 2015. Biology and ecology of Radiolaria. In S. Ohtsuka et al. eds.): *Marine protists.* Tokyo: Springer.

Swanberg N.R. & Bjørklund K.R. 1986. The radiolarian fauna of western Norwegian fjords: patterns of abundance in the plankton. *Marine Micropaleontology 11*, 231–241, doi: 10.1016/0377-8398(86)90017-4.

Swanberg N.R. & Bjørklund K.R. 1987. Radiolaria in the plankton of some fjords in western and northern Norway: the distribution of species. *Sarsia 72*, 231–244, doi: 10.1080/00364827.1987.10419720.

Swanberg N.R. & Bjørklund K.R. 1992. The radiolarian fauna of western Norwegian fjords: a multivariate comparison of the sediment and plankton assemblages. *Micropaleontology 38(4)*, 57–74, doi: 10.2307/1485843.

Swanberg N.R. & Eide L.K. 1992. The radiolarian fauna at the ice edge in the Greenland Sea during summer, 1988. *Journal of Marine Research 50*, 297–320, doi: 10.1357/002224092784797674.

Takahashi K. 1991. Mineral flux and biogeochemical cycles of marine planktonic protozoa—session summary. In P.C. Reid et al. (eds.): *Protozoa and their role in marine processes*. Pp. 347–359. Berlin: Springer.

Takahashi K. & Anderson O.R. 2002. Class Phaeodaria. In J.J. Lee et al. (eds.): *The second illustrated guide to the Protozoa.* Pp. 981–994. Lawrence, KS: Society of Protozoologists.

Citation: *Polar Research* 2023, *42*, 9584, http://dx.doi.org/10.33265/polar.v42.9584

Takahashi K., Hurd D.C. & Honjo S. 1983. Phaeodarian skeletons: their role in silica transport to the deep sea. *Science 222*, 616–618, doi: 10.1126/science.222.4624.616.

Takahashi K. & Ling H.Y. 1980. Distribution of *Sticholonche* (Radiolaria) in the upper 800 m of the waters in the Equatorial Pacific. *Marine Micropaleontology 5*, 311–319, doi: 10.1016/0377-8398(80)90015-8.

Tan Z.Y., Gao H.Z. & Su X.H. 1978. The quantitative distribution of *Sticholonche zanclea* in the western part of the East China Sea. *Oceanologia et Limnologia Sinica 9*, 59–66. (In Chinese, with English abstract.)

Wassmann P., Svendsen H., Keck A. & Reigstad M. 1996. Selected aspects of the physical oceanography and particle fluxes in fjords of northern Norway. *Journal of Marine Systems 8*, 53–71, doi: 10.1016/0924-7963(95)00037-2.

Welling L.A. 1996. *Environmental control of radiolarian abundance in the central Equatorial Pacific and implications for paleoceanographic reconstructions*. PhD thesis, Oregon State University, Corvallis.

Yuasa T., Dolven J.K., Bjørklund K.R., Mayama S. & Takahashi O. 2009. Molecular phylogenetic position of *Hexacontium pachydermum* Jørgensen (Radiolaria). *Marine Micropaleontology* 73, 129–134, doi: 10.1016/j.marmicro.2009.08.001.

Yuasa T., Takahashi O., Dolven J.K., Mayama S., Matsuoka A., Honda D. & Bjørklund K.R. 2006. Phylogenetic position of the small solitary phaeodarians (Radiolaria) based on 18S rDNA sequences by single cell PCR analysis. *Marine Micropaleontology 59*, 104–114, doi: 10.1016/j.marmicro.2006.01.003.